

Implantation of rAAV5-IGF-I Transduced Autologous Chondrocytes Improves Cartilage Repair in Full-thickness Defects in the Equine Model

Kyla F Ortvad¹, Laila Begum¹, Hussni O Mohammed² and Alan J Nixon¹

¹Comparative Orthopaedics Laboratory, Cornell University, Ithaca, New York, USA; ²Department of Population Medicine and Diagnostic Sciences, College of Veterinary Medicine, Cornell University, Ithaca, New York, USA

Cartilage injury often precipitates osteoarthritis which has driven research to bolster repair in cartilage impact damage. Autologous chondrocytes transduced with rAAV5-IGF-I were evaluated in chondral defects in a well-established large animal model. Cartilage was harvested from the talus of 24 horses; chondrocytes were isolated and stored frozen. Twenty million cells were cultured and transduced with 10^5 AAV vg/cell prior to implantation. Chondrocytes from eight horses were transduced with rAAV5-IGF-I, chondrocytes from eight horses with rAAV5-GFP, and chondrocytes from eight horses were not transduced. A 15 mm full-thickness chondral defect was created arthroscopically in the lateral trochlear ridge of the femur in both femoropatellar joints. Treated defects were filled with naive or gene-enhanced chondrocytes, in fibrin vehicle. Control defects in the opposite limb received fibrin alone. rAAV5-IGF-I transduced chondrocytes resulted in significantly better healing at 8 week arthroscopy and 8 month necropsy examination when compared to controls. At 8 months, defects implanted with cells expressing IGF-I had better histological scores compared to control defects and defects repaired with naive chondrocytes. This included increased chondrocyte predominance and collagen type II, both features of hyaline-like repair tissue. The equine model closely approximates human cartilage healing, indicating AAV-mediated genetic modification of chondrocytes may be clinically beneficial to humans.

Received 7 February 2014; accepted 2 October 2014; advance online publication 2 December 2014. doi:10.1038/mt.2014.198

INTRODUCTION

Damaged articular cartilage often precipitates painful and debilitating osteoarthritis.¹ Joint injury and osteoarthritis are often career-ending in athletes and are one of the most common causes of disability in the aging population. Cartilage has minimal to no intrinsic healing capabilities,² prompting investigation of a variety of methods to improve repair. Full-thickness lesions that are left untreated fill with fibrous tissue which is biochemically

and biomechanically inferior to hyaline cartilage.³ Techniques to improve cartilage repair have been investigated including marrow stimulation,⁴ osteochondral transplantation (mosaicplasty),⁵ and more recently autologous chondrocyte implantation.⁶ Cell-based cartilage repair has shown promising long-term results in equine and human patients with production of hyaline-like repair tissue following transplantation of chondrocytes into chondral defects.⁷ However, repair tissue may be further improved through the genetic manipulation of the donor chondrocytes.

Previous chondrocyte transplantation studies in the equine model have used allogeneic chondrocytes from juvenile donors⁸ as these cells are easily accessible from donor animals, limit treatment to one surgical event and decrease donor site morbidity. However, the potential detrimental effect of the host immune response on healing continues to be of concern. Although chondrocytes are generally considered to be immunoprivileged when contained in the extracellular matrix (ECM),⁹ they express MHC I and II¹⁰ and could incite an immune response. Use of autologous chondrocytes eliminates potential immune responses to cells, which could benefit overall repair.

Insulin-like growth factor-I (IGF-I) has been identified as a critical anabolic and mitogenic protein in chondrocyte metabolism and cartilage repair.¹¹ IGF-I increases aggrecan and collagen type II content in chondrocyte cultures, including explants, monolayer and three-dimensional systems, as well as enhancing the repair potential of chondrocytes grafted into cartilage lesions in horses.^{12,13} Additionally, it has been suggested that IGF-I plays a role in the healing of damaged cartilage as it partially protects and aids in the recovery of the ECM following experimentally induced damage with IL-1 and TNF- α .^{14,15} Although chondrocytes supplemented with exogenous IGF-I have been used in clinical practice,¹⁶ the transitory nature of growth factor supplementation has led to investigation of gene therapy approaches.

Viral vectors including adenovirus and retrovirus have been examined for musculoskeletal gene therapy due to high transduction efficiencies but concerns regarding immunogenicity and genome integration have limited their use. Adeno-associated virus (AAV) may be a more feasible and clinically relevant vector as it lacks pathogenicity, can transduce dividing and nondividing cells, has long-term transgene expression, and transduced

Correspondence: Alan J Nixon, Cornell University, Ithaca, New York, USA. E-mail: ajn1@cornell.edu

cells appear to be minimally immunogenic.¹⁷ Recombinant AAVs are not capable of productive infections and rarely integrate into host genomes. AAV, being a single-stranded DNA virus, requires second strand synthesis of the viral genome prior to transcription and expression of transgenes. More recently a self-complementary AAV (scAAV) has been developed to decrease the lag time between transduction and transgene expression, as the genome can fold into dsDNA without the need for second strand synthesis.¹⁸

The objective of this study was to evaluate short- and long-term cartilage healing in full-thickness chondral defects repaired with autologous chondrocytes transduced *ex vivo* with a scAAV5 vector overexpressing IGF-I. We hypothesized that autologous chondrocytes overexpressing IGF-I would improve articular

cartilage healing, including morphologic, histologic, and biochemical parameters.

RESULTS

Arthroscopic cartilage harvest yielded autologous chondrocytes for grafting

Arthroscopic cartilage harvest of the non-weight-bearing regions of the distal surfaces of the medial and lateral trochlear ridges of the talus was achieved in each horse ($n = 24$) yielding 1.5–2.5 g of cartilage. Collagenase digestion of cartilage produced $\sim 15 \times 10^6$ chondrocytes. Full-thickness chondral defects were created successfully in the lateral trochlear ridge of both femurs using an arthroscopically guided 15 mm diameter fluted spade-bit cutter (Figure 1a). Calcified cartilage was completely debried from

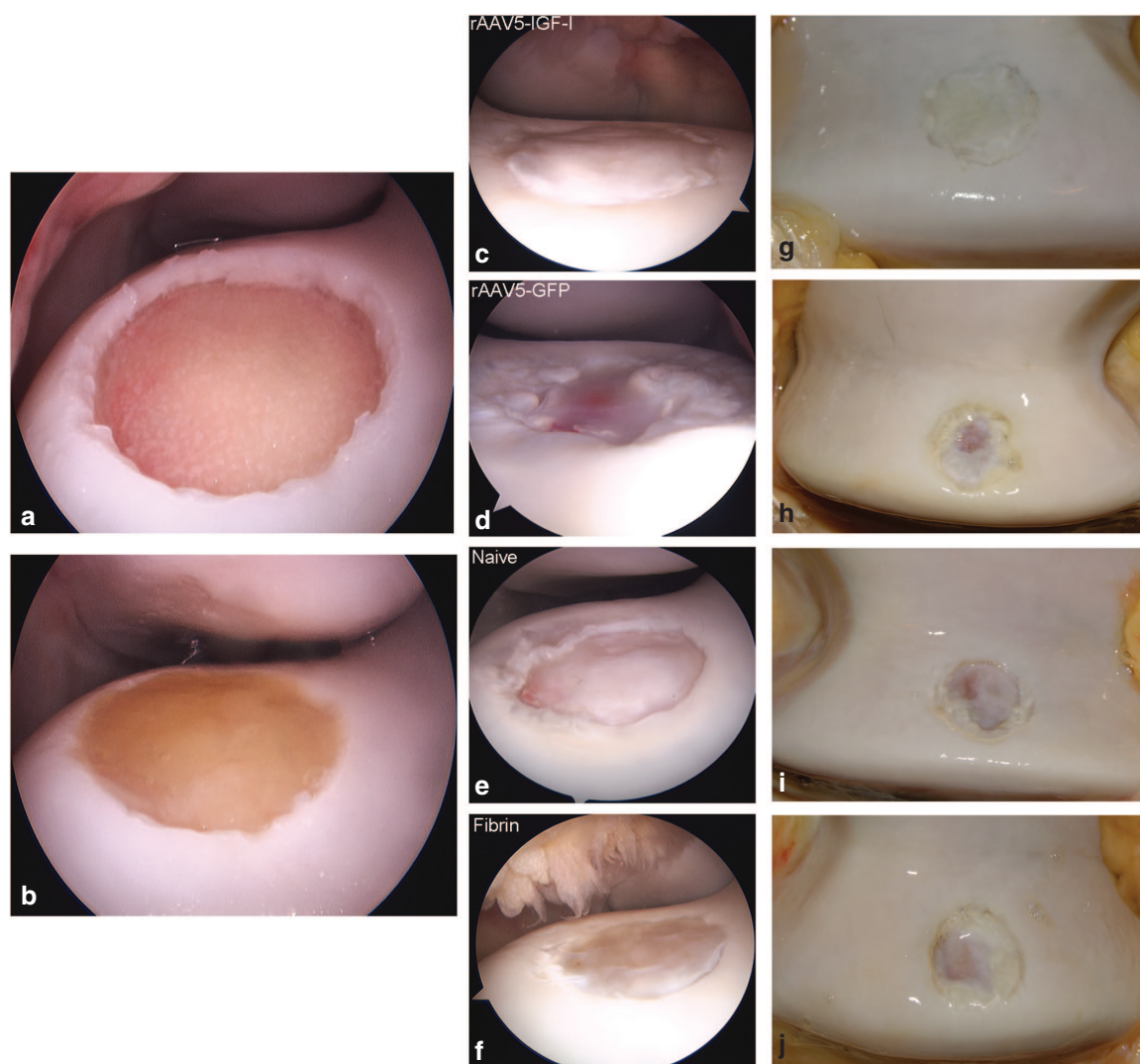


Figure 1 Arthroscopic and gross images of 15-mm diameter full-thickness chondral defects in the lateral trochlear ridge of the femur at (a,b) time of implantation, (c–f) 8 weeks postimplantation, and (g–j) 8 months postimplantation. (a) A full-thickness, 15-mm-diameter chondral defect in the lateral trochlear ridge of the femur prior to implantation. (b) The same defect after chondrocyte implantation. The implant has been stabilized by polymerization of the fibrin vehicle. (c) Defect repaired with rAAV5-IGF-I transduced chondrocytes 8 weeks postimplantation, showing good defect fill and white “cartilage-like” tissue compared to the defects filled with (d) rAAV5-GFP transduced chondrocytes, (e) naive chondrocytes, or (f) fibrin alone. (g–j) Gross images of the same defects at 8 months postimplantation are shown. (g) Gross appearance of a defect repaired with rAAV5-IGF-I transduced chondrocytes compared to (h) a defect repaired with rAAV5-GFP, (i) a defect repaired with naive chondrocytes, and (j) a defect repaired with fibrin alone.

the surface of the defect using a curette. Horses were randomly assigned to a treatment group in which one chondral defect was filled with (i) fibrin-containing chondrocytes transduced with rAAV5-IGF-I ($n=8$), (ii) fibrin-containing chondrocytes transduced with rAAV5-GFP (positive control) ($n = 8$), or (iii) fibrin containing naive, untransduced chondrocytes ($n = 8$). The defects were filled with 20×10^6 cells, while the contralateral joint of each horse was grafted with the autogenous fibrin vehicle alone ($n = 24$). All grafts stabilized within several minutes and remained stable while joints were moved through range of motion (**Figure 1b**).

Abundant IGF-I gene expression from chondrocytes transduced *in vitro* with the rAAV5-IGF-I vector was confirmed in preliminary experiments.¹⁹ This previously published qPCR data showed that at 14 days posttransduction, expression of IGF-I in chondrocytes transduced with 1×10^5 vg/cell was 115-fold higher than expression of IGF-I in untransduced cells. IGF-I concentration in the supernatants of rAAV5-IGF-I transduced chondrocyte cultures was also significantly increased at 14 days posttransduction (55.7 ± 8.5 ng/ml), compared to untransduced cells (0.24 ± 0.1 ng/ml).¹⁹

Chondral defects repaired with rAAV5-IGF-I transduced chondrocytes had improved healing at 8 weeks and 8 months

Short-term healing of the defects was assessed arthroscopically at 8 weeks postimplantation, at which time all defects were variably filled with repair tissue. Representative images from second-look arthroscopy from all four treatment groups are shown (**Figure 1c–f**). Healing was evaluated using a pathology scoring system based on five parameters yielding independent scores for each category and a composite score (**Table 1**). Pathology scores closest to zero reflected repair tissue most similar to native cartilage, while higher scores reflected the most abnormal repair tissue. Defects repaired with rAAV5-IGF-I transduced chondrocytes had improved coverage with smooth repair tissue (**Figure 1c**), compared to defects repaired with rAAV5-GFP chondrocytes (**Figure 1d**) or fibrin alone (**Figure 1f**), and this was reflected by rAAV5-IGF-I defects having significantly lower (better) pathology scores (**Table 2**). Additionally, rAAV5-IGF-I treated defects had significantly more white repair tissue (**Figure 1c**) compared to defects repaired with rAAV5-GFP chondrocytes (**Figure 1d**) or fibrin alone (**Figure 1f**). Overall, defects repaired with chondrocytes overexpressing IGF-I had significantly lower total arthroscopic pathology scores (mean \pm SEM; 5.35 ± 1.30) compared to defects filled with rAAV5-GFP (11.05 ± 1.30) and fibrin alone (10.79 ± 0.73). The difference between the total pathology score for naive chondrocytes (8.56 ± 1.30) and rAAV5-IGF-I treated defects did not reach significance (**Table 2**).

Long-term healing of defects was assessed at 8 months postimplantation by gross pathology scores (**Table 1**), histology and immunohistology, and biochemical characterization. Gross images of healing defects from the four treatment groups (**Figure 1g–j**) revealed improved repair in IGF-I expressing chondrocyte implanted defects. Individual parameter and total gross scores presented in **Table 3** show defects repaired with rAAV5-IGF-I chondrocytes had significantly lower (better) total pathology scores (mean \pm SEM, 4.13 ± 0.69), compared to defects

repaired with naive chondrocytes (6.99 ± 0.69) and fibrin alone (6.75 ± 0.39). Chondrocyte-IGF-I implanted defects had improved total pathology scores compared to defects treated with chondrocytes expressing GFP (5.75 ; SE ± 0.69), but this difference did not reach significance.

Osteochondral sections of repair tissue were also scored using a semi-quantitative histologic scoring system (**Table 1**). Histologic scores were superior in chondrocyte-IGF-I implanted defects, following the same pattern of improvement evident in gross pathology scores. Representative images of all four treatment groups are shown (**Figure 2a–d**) and individual parameter and total pathology scores are shown in **Table 4**. Total pathology scores were significantly improved for defects implanted with chondrocytes expressing IGF-I (mean \pm SEM, 12.47 ± 1.26), compared to defects treated with naive chondrocytes (18.32 ± 1.26) or fibrin alone (18.58 ± 0.77) (**Table 4**). Although total pathology scores from defects repaired with chondrocytes expressing IGF-I (12.47 ± 1.26) were better than those repaired with chondrocytes expressing an irrelevant gene (GFP) (15.97 ± 1.26), these differences were not statistically significant (**Table 4**).

rAAV5-IGF-I transduced chondrocytes increase synovial fluid IGF-I concentration

In order to assess functional transgene expression following chondrocyte implantation, IGF-I content in the synovial fluid of femoropatellar joints was analyzed over time using a mixed effects model to account for repeated measures. The effect of day ($P < 0.0001$) and treatment group ($P < 0.012$) were both significant, as was the interaction between day and treatment groups ($P < 0.004$). IGF-I content in the synovial fluid increased in all treatment groups immediately postoperatively with return to baseline by day 56 (**Figure 3a**). Synovial fluid IGF-I concentrations obtained from femoropatellar joints implanted with chondrocytes overexpressing IGF-I was significantly increased over joints treated with chondrocytes expressing GFP ($P = 0.025$) and fibrin alone ($P < 0.0001$) at day 4 (**Figure 3a**). At day 7 postoperatively, synovial IGF-I concentrations in joints treated with chondrocytes expressing IGF-I were still significantly increased over joints implanted with GFP expressing chondrocytes ($P = 0.014$) and fibrin alone ($P = 0.0006$) (**Figure 3a**). IGF-I levels were highest 4 days postoperatively with rAAV5-IGF-I gene enhanced joints having 202.4 ng/ml (± 24.4) compared to 145.3 ng/ml (± 17.7) in joints implanted with chondrocytes expressing GFP, 172.2 ng/ml (± 85.4) in naive chondrocyte joints, and 125.7 ng/ml (± 12.9) in fibrin joints (**Figure 3a**).

The correlation between IGF-I concentrations in femoropatellar synovial fluid and healing of defects was also evaluated. There was a weak, but significant ($P < 0.05$), correlation between peak IGF-I concentrations at day 4 and 7 with 8 week arthroscopic pathology scores, 8 month gross pathology scores, and total histological pathology scores. Horses with higher IGF-I concentrations postimplantation had lower pathology in the short and long term.

Further analysis of synovial fluid composition was performed to assess the inflammatory response of the joint to the vectors. The nucleated cell count (NCC) increased over baseline in femoropatellar joints of all treatment groups 4 days postoperatively; however, these increases were only significantly different compared to preoperative NCCs in horses treated with

Table 1 Pathology scoring system for arthroscopic and gross tissue pathology (0 = Normal cartilage; 20 = Most abnormal) and for histological tissue pathology. (0 = Normal cartilage; 31 = Most abnormal)

Arthroscopic and gross tissue pathology score parameter	Qualifications (%)	Histological healing score parameter	Qualifications (%)
Defect fill		Defect fill	
0	100	0	100
1	>75; >100	1	>75; >100
2	51–75	2	51–75
3	26–50	3	26–50
4	0–25	4	0–25
Amount of smooth repair tissue covering defect		Chondrocyte predominance	
0	100	0	All
1	>75	1	67–99
2	51–75	2	34–66
3	26–50	3	1–33
4	0–25	4	None
Amount of white tissue		Perilesional cloning	
0	100	0	None
1	>75	1	Seldom
2	51–75	2	Occasional
3	26–50	3	Frequent
4	0–25		
Graft–recipient tissue integration		Lesion–perilesion tissue integration	
0	100	0	Complete
1	>75	1	Gap on one side
2	51–75	2	Gap on both sides
3	26–50		
4	0–25		
Subchondral bone attachment		Subchondral bone attachment	
0	100	0	100
1	>75	1	>75
2	51–75	2	51–75
3	26–50	3	26–50
4	0–25	4	0–25
		Surface fibrillation	
		0	None
		1	Slight fibrillation
		2	Moderate fibrillation
		3	Severe fibrillation
		Tidemark reformation	
		0	Complete
		1	51–99
		2	1–50
		3	None
		Toluidine blue staining	
		0	91–100
		1	76–90
		2	51–75
		3	26–50
		4	0–25
		Collagen type II predominance	
		0	>90
		1	76–90
		2	51–75
		3	26–50
		4	0–25

Table 2 Arthroscopic healing scores of lesions at 8 week second look arthroscopy

Treatment group	Smoothness of repair tissue	Defect fill	Tissue color	Graft–recipient tissue integration	Subchondral bone attachment	Total score
rAAV5-IGF-I	1.58 ± 0.32 ^a	1.36 ± 0.35	1.51 ± 0.32 ^a	0.73 ± 0.32	0.35 ± 0.42	5.35 ± 1.30 ^a
rAAV5-GFP	3.10 ± 0.32 ^b	2.51 ± 0.35	2.87 ± 0.32 ^b	1.54 ± 0.32	0.93 ± 0.42	11.05 ± 1.30 ^b
Naive chondrocyte	2.32 ± 0.32 ^{ab}	2.25 ± 0.35	2.62 ± 0.32 ^{ab}	0.85 ± 0.32	0.46 ± 0.42	8.56 ± 1.30 ^{ab}
Fibrin	3.12 ± 0.18 ^b	2.38 ± 0.20	2.96 ± 0.18 ^b	1.08 ± 0.20	1.25 ± 0.24	10.79 ± 0.73 ^b

Data presented as mean ± SEM. Results analyzed using a mixed effects model with horse as a random effect. Different letters denote significant differences between groups. $n = 8$ (rAAV5-IGF-I, rAAV5-GFP, naive), $n = 24$ (fibrin); $P < 0.05$.

Table 3 Gross healing scores of lesions at 8 months postimplantation

Treatment group	Smoothness of repair tissue	Defect fill	Tissue color	Graft–recipient tissue integration	Subchondral bone attachment	Total score
rAAV5-IGF-I	1.13 ± 0.24 ^a	0.87 ± 0.23	1.13 ± 0.26	0.81 ± 0.27 ^a	0.25 ± 0.27	4.13 ± 0.69 ^a
rAAV5-GFP	1.63 ± 0.24 ^{ab}	1.53 ± 0.23	1.25 ± 0.26	0.89 ± 0.27 ^a	0.53 ± 0.27	5.75 ± 0.69 ^{ab}
Naive chondrocyte	2.13 ± 0.24 ^b	1.60 ± 0.23	1.75 ± 0.25	0.96 ± 0.27 ^{ab}	0.48 ± 0.27	6.99 ± 0.69 ^b
Control	1.50 ± 0.14 ^{ab}	1.29 ± 0.13	1.54 ± 0.14	1.67 ± 0.16 ^b	0.96 ± 0.27	6.75 ± 0.39 ^b

Data presented as mean ± SEM. Results analyzed using a mixed effects model with horse as a random effect. Different letters denote significant differences between groups. $n = 8$ (rAAV5-IGF-I, rAAV5-GFP, naive), $n = 24$ (fibrin); $P < 0.05$.

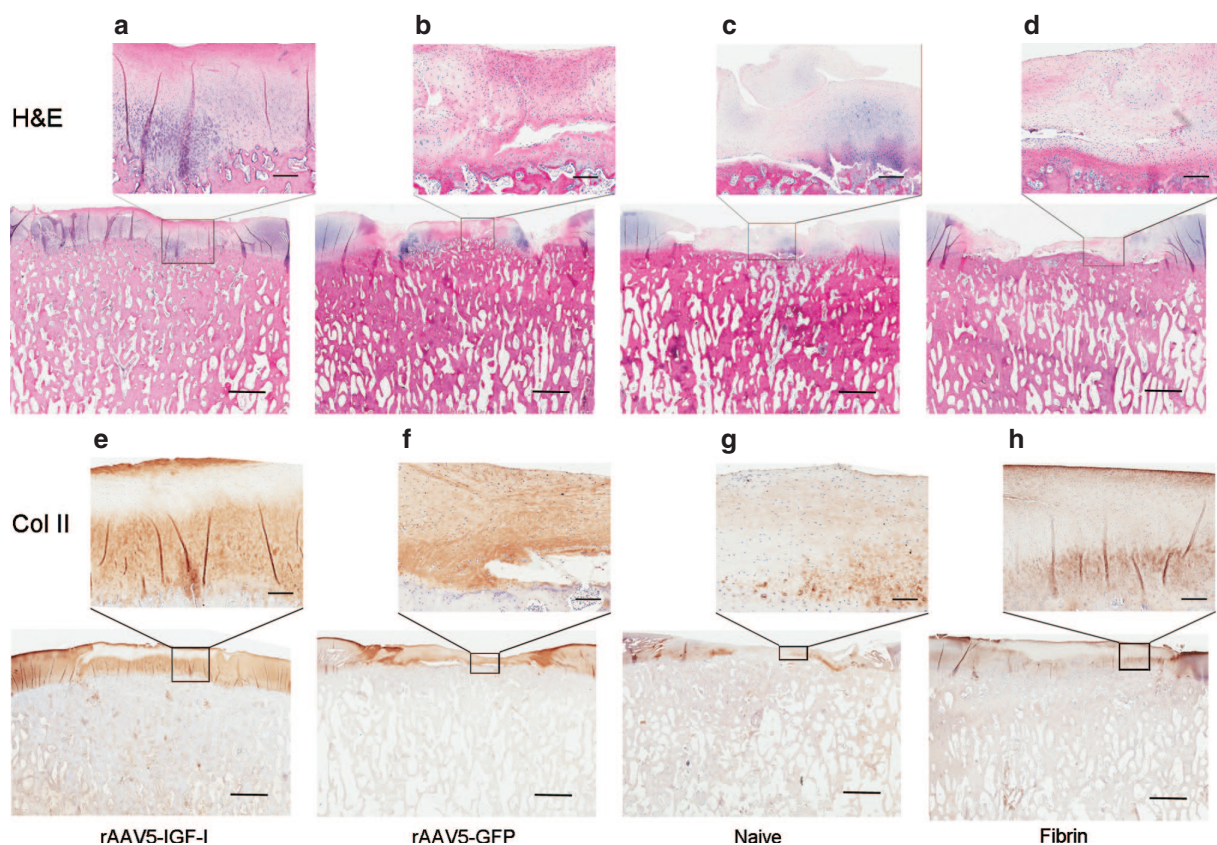


Figure 2 Photomicrographs of osteochondral sections taken from repair tissue at 8 months postimplantation showing (a–d) tissue architecture and (e–h) collagen type II formation. (a) rAAV5-IGF-I transduced chondrocytes formed tissue with a chondrocyte predominance, improved tissue organization, and less fibrous tissue than defects treated with either (b) rAAV5-GFP transduced chondrocytes, (c) naive chondrocytes, or (d) fibrin alone. (e) rAAV5-IGF-I transduced chondrocytes show increased collagen type II (brown staining) compared to defects repaired with (f) rAAV5-GFP transduced chondrocytes, (g) naive chondrocytes, or (h) fibrin alone. (Bar = 5 mm; inset bar = 500 μ m).

rAAV5-GFP chondrocytes ($4,712.5 \pm 1,366.8$ cells/ μ l) and fibrin alone ($3,890.5 \pm 709.8$ cells/ μ l) (Figure 3b). Horses treated with GFP-expressing chondrocytes had a significantly higher NCC 4 days postoperatively compared to horses implanted

with chondrocytes expressing IGF-I ($2,616.7 \pm 360.0$ cells/ μ l; $P = 0.0042$) and naive chondrocytes ($2,871.4 \pm 260.7$ cells/ μ l; $P = 0.015$) (Figure 3b). All NCCs decreased by day 7 postoperatively, with no significant differences between pre- and

Table 4 Histologic healing scores of lesions at 8 months postimplantation

Treatment group	Defect filling (%)	Chondrocyte predominance	Perilesion cloning	Subchondral bone		Perimeter attachment	Surface fibrillation	Tidemark	Toluidine blue staining %	Collagen type II IHC	Total score
				attachment	attainment						
rAAV5-IGF-I	0.92 ± 0.42	1.76 ± 0.22 ^a	0.35 ± 0.2 ^a	0.65 ± 0.47	0.57 ± 0.22	0.58 ± 0.29	2.25 ± 0.17 ^a	3.23 ± 0.2 ^a	2.09 ± 0.33 ^a	12.47 ± 1.26 ^a	
rAAV5-GFP	1.53 ± 0.42	2.38 ± 0.22 ^{ab}	0.5 ± 0.22 ^a	1.30 ± 0.47	0.82 ± 0.22	1.02 ± 0.29	2.25 ± 0.17 ^a	3.50 ± 0.2 ^{ab}	2.63 ± 0.33 ^{ab}	15.97 ± 1.26 ^{ab}	
Naive chondrocyte	1.55 ± 0.42	2.49 ± 0.22 ^{ab}	0.78 ± 0.22 ^{ab}	1.30 ± 0.47	1.23 ± 0.22	1.52 ± 0.29	2.63 ± 0.17 ^{ab}	3.90 ± 0.2 ^{ab}	3.02 ± 0.33 ^{ab}	18.32 ± 1.26 ^b	
Fibrin	1.25 ± 0.25	2.71 ± 0.12 ^b	1.25 ± 0.12 ^b	1.08 ± 0.27	1.08 ± 0.13	1.29 ± 0.18	2.88 ± 0.9 ^b	3.88 ± 0.11 ^b	3.17 ± 0.19 ^b	18.58 ± 0.77 ^b	

Data presented as mean ± SEM. Results analyzed using a mixed effects model with horse as a random effect. Different letters denote significant differences between groups. $n = 8$ (rAAV5-IGF-I, rAAV5-GFP, naive), $n = 24$ (fibrin); $P < 0.05$. IHC, immunohistochemistry.

postoperative counts. Synovial total protein levels increased significantly over baseline in all femoropatellar joints immediately following surgery, with no significant differences between treatment groups (Figure 3c). Total protein concentrations remained significantly elevated above preoperative levels until day 56 postoperatively in all groups except those implanted with chondrocytes expressing IGF-I, in which total protein concentrations returned to baseline by day 28 (Figure 3c).

Chondrocytes transduced with rAAV5-IGF-I improved biochemical properties of repair defects

Representative images of collagen type II immunoreaction in Figure 2e-h indicated more collagen type II in IGF-I treated defects compared to other treatment groups. Scoring of immunohistological sections supported this finding, with more collagen type II content in chondrocyte-IGF-I treated defects, although these differences were only statistically significant when compared to fibrin-treated defects (Table 4). Increased collagen type II content in chondrocyte-IGF-I implanted defects was confirmed by ELISA, with significantly more collagen type II in IGF-I treated defects compared to all other treatment groups ($P < 0.005$) (Figure 4).

Proteoglycan content (μg glycosaminoglycan/mg dry weight cartilage) of repair tissue at 8 months postimplantation was significantly higher in defects repaired with chondrocytes overexpressing IGF-I (mean ± SEM; $24.5 \pm 2.32 \mu\text{g}/\text{mg}$) compared to GFP-treated defects ($14.5 \pm 2.48 \mu\text{g}/\text{mg}$). However, there were no significant differences in proteoglycan between chondrocyte-IGF-I, naive chondrocytes ($19.0 \pm 2.30 \mu\text{g}/\text{mg}$), and fibrin-treated defects ($23.3 \pm 1.43 \mu\text{g}/\text{mg}$) (Table 5). Interestingly, sections from defects implanted with chondrocytes expressing IGF-I had the most toluidine blue staining on histochemical analysis, although these differences were only significant between chondrocyte-IGF-I treated defects and fibrin-treated defects (Table 4). Across all four treatment groups, proteoglycan content in repair tissue ($20.3 \pm 2.46 \mu\text{g}/\text{mg}$) was $\sim 1/3$ the amount of proteoglycan content present in perilesion ($67.4 \pm 2.53 \mu\text{g}/\text{mg}$) and remote cartilage ($63.9 \pm 1.63 \mu\text{g}/\text{mg}$), indicating moderate regeneration of the ECM at 8 months. There were no differences in DNA content of repair tissue across the four treatment groups (Table 5). Repair tissue DNA content was less than that of perilesion or remote tissues in all four groups indicating that repair tissue had decreased cellularity compared to native cartilage (Table 5).

Expression of genes associated with hyaline cartilage including IGF-I, aggrecan, collagen type II, and collagen type I were assessed in repair tissue, perilesion tissue, and remote tissue by qRT-PCR. At 8 months postimplantation, there were no differences in expression of IGF-I, aggrecan, collagen type II, or collagen type I in repair tissue from defects repaired with chondrocytes overexpressing IGF-I or GFP, naive chondrocytes, or fibrin vehicle alone (Supplementary Figure S1). No differences in gene expression were noted in the perilesion or remote tissue between any of the treatment groups.

rAAV5 did not cause a significant inflammatory response in synovium

Synovial biopsies were collected during arthroscopic examination at 8 weeks postimplantation and at 8 months postimplantation.

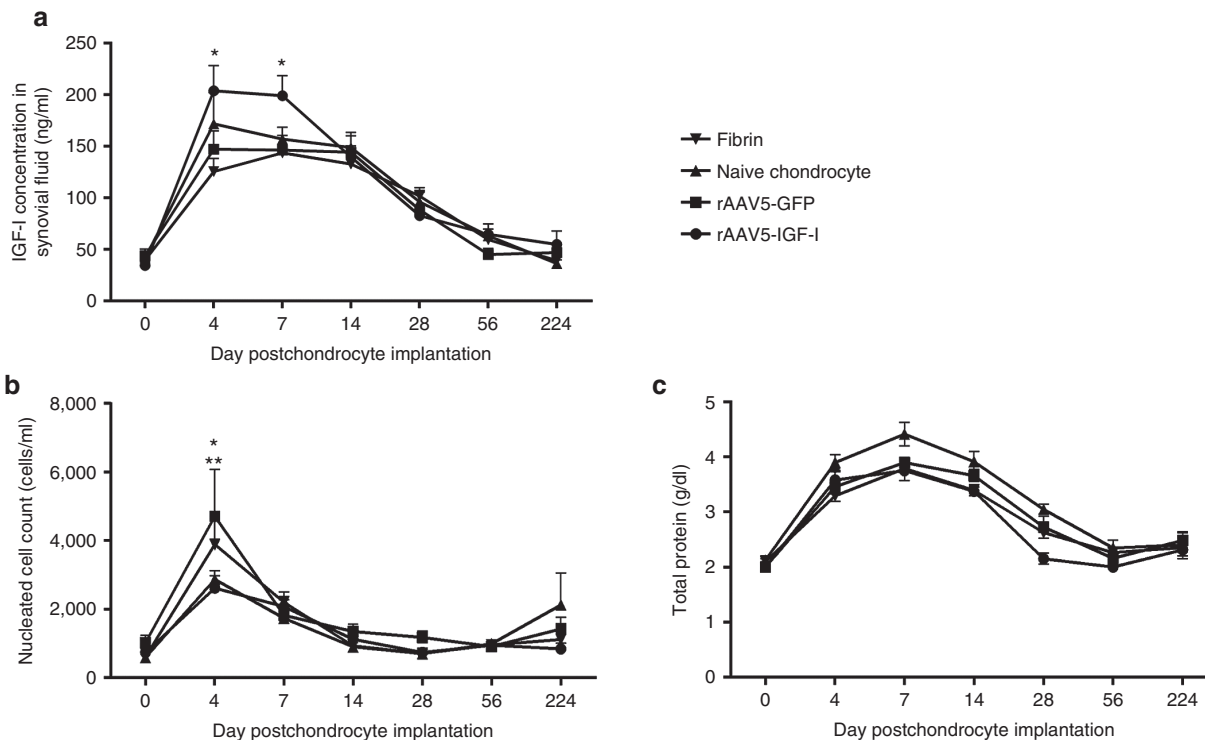


Figure 3 Femoropatellar IGF-I concentration and synovial fluid composition (mean ± SEM) over time following chondrocyte implantation. **(a)** IGF-I concentration in the synovial fluid of joints treated with rAAV5-IGF-I transduced chondrocytes was significantly increased over rAAV5-GFP treated joints or fibrin-treated joints at days 4 and 7 (**P* < 0.05). **(b)** Nucleated cell count (NCC) was significantly increased over baseline in rAAV5-GFP and fibrin-treated joints at day 4 (**P* < 0.05). NCC in rAAV5-GFP treated joints was also significantly increased over joints treated with rAAV5-IGF-I chondrocytes and naive chondrocytes at day 4 (***P* < 0.05). **(c)** Total protein (g/dl) increased in all treatment groups postoperatively with no significant differences between groups.

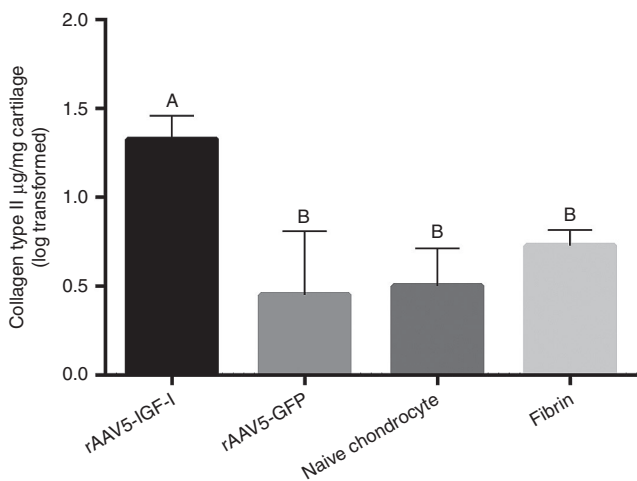


Figure 4 Log transformed (±SEM) collagen type II content in repair tissue in rAAV5-IGF-I, rAAV5-GFP, naive chondrocyte, and fibrin treated (control) defects. Tukey’s classification letters indicate significant differences between treatment groups.

Synovium was evaluated and scored for changes in villus architecture, subintimal fibrosis, intimal thickening, increased vasculature, or inflammatory cell infiltration indicative of an inflammatory response. Synovial biopsy scores showed no significant differences between treatment groups at either 8 weeks or 8 months. Cartilage repair with chondrocytes transduced with rAAV5 did not appear

Table 5 Biochemical analysis of lesion cartilage 8 months postimplantation

Treatment group	Glycosaminoglycan (µg/mg)	DNA (µg/mg)
rAAV5-IGF-I	24.5 (2.32) ^a	7.34 (1.30)
rAAV5-GFP	14.5 (2.48) ^b	4.34 (1.14)
Naive chondrocytes	19.0 (2.30) ^{ab}	5.82 (1.30)
Fibrin	23.3 (1.43) ^{ab}	7.32 (0.71)

Data presented as mean ± SEM. Results analyzed using a mixed effects model with horse as a random effect. Different letters denote significant differences between groups. *P* < 0.05.

to cause a significant inflammatory reaction in the synovial tissue of the femoropatellar joint, consistent with the synovial fluid profiles observed between the groups. Biopsies of the ileofemoral and popliteal lymph nodes (main draining lymph nodes of the femoropatellar joints) taken at necropsy showed significantly more reaction in ileofemoral than popliteal lymph nodes within all treatment groups; however, no differences were noted in lymph node reactivity between any of the treatment groups.

DISCUSSION

Implantation of autologous chondrocytes transduced with rAAV5-IGF-I *ex vivo* resulted in improved repair of full-thickness chondral defects in the horse model, both in the short term (8 weeks postimplantation) and long term (8 months postimplantation).

These grafted defects showed features of hyaline-like repair tissue including hyaline-like tissue architecture, chondrocyte predominance, and collagen type II abundance. The total histologic scores of chondrocyte-IGF-I treated defects were significantly improved over defects implanted with naive chondrocytes or fibrin vehicle alone. Collagen type II immunohistochemistry scores were also significantly improved in IGF-I-enhanced repairs compared to defects treated with fibrin alone. These results were further validated by collagen type II ELISA which showed significantly increased collagen type II protein in IGF-I treated defects compared to defects implanted with chondrocytes expressing an inconsequential GFP gene or in defects grafted with fibrin alone. Upregulation of collagen type II synthesis by chondrocytes exposed to IGF-I has been shown previously.^{20,21} The increased collagen type II levels in our study are likely due to overexpression of IGF-I by the rAAV-IGF-I vector.

IGF-I has been shown to play a major role in articular cartilage homeostasis and anabolism.^{14,22} Previous studies in large animal cartilage repair models showed the addition of exogenous IGF-I to chondrocyte grafts improved repair of chondral defects *in vivo*. However, persisting fibrous tissue in the surface layers of the repair at 8 months suggested inadequate persistence of the growth factor in the repair tissue, or excessive loss of chondrocytes or IGF-I from the surface layers of the new cartilage.¹² In the current study, gene transduction of transplanted chondrocytes was used to increase longevity of IGF-I supplementation in repair tissue. Significantly increased levels of IGF-I protein were noted in the synovial fluid of joints implanted with chondrocytes expressing the IGF-I gene at 4 and 7 days postimplantation, suggesting active transgene expression. Interestingly, there was a significant correlation between IGF-I concentrations at days 4 and 7, and healing at 8 weeks and 8 months; horses with higher IGF-I concentrations postimplantation were more likely to have superior healing.

The decrease in synovial fluid IGF-I concentration after day 7 was expected, as the femoropatellar joint is a voluminous joint, and the chondral defect containing transduced cells was relatively small. The inevitable dilution of IGF-I produced by transduced cells would make increases in IGF-I protein difficult to detect unless they were quite large. Expression profiles from chondrocytes transduced *in vitro* with rAAV5-IGF-I showed significantly elevated IGF-I concentrations up to 28 days.¹⁹ Alternatively, it is possible that IGF-I excretion into the synovial fluid was reduced due to early cessation of transgene expression, premature death of implanted chondrocytes, or maturation of the graft leading to decreased permeability and subsequent loss of IGF-I to the joint fluid. Additionally, loss of transgene expression can occur due to cytotoxic T-cell responses that destroy transduced cells. Although there did not appear to be a significant inflammatory response in treated joints, specific immune responses were beyond the scope of this study and should be considered as a potential cause of loss of transgene expression in future experiments. Repair tissue collected at 8 months postimplantation from the four treatment groups did not show any significant differences in IGF-I transcriptional activity based on qPCR which supports loss of transgene overexpression in the long term. Biopsies of repair tissue at earlier time points could shed light on the longevity of IGF-I expression; however, disruption of the repair site is a major concern with serial biopsy procedures.

AAV has been touted as an ideal viral vector due to its lack of pathogenicity, ability to transduce nondividing cells, and prolonged expression.¹⁷ Tissue tropism has been shown for several AAV serotypes, and these affinities are likely species specific. rAAV5 provided excellent transduction of equine chondrocytes in this study, based on evidence from fluorescent microscopy showing GFP expression in preimplantation monolayer cultures. Other serotypes, including rAAV2, have been evaluated for transduction efficiency of articular cells; however, preliminary data in our laboratory comparing rAAV2 and rAAV5 revealed optimal transduction of chondrocytes by rAAV5 at a dose of 10^5 vg/cell.¹⁹ Although defects repaired with chondrocytes expressing IGF-I had better gross and histological pathology scores at 8 months compared to naive chondrocyte repairs, the improvement compared to defects implanted with chondrocytes expressing a null gene (GFP) did not achieve statistical differences. It is possible that rAAV5 transduction alone played a role in healing of defects. AAV vectors have a multitude of intracellular effects, many of which remain unknown. Given this, it is possible that simple AAV transduction could enhance healing capabilities of chondrocytes.

In the past, similar studies in the horse have used allogeneic chondrocytes as a source for cell-based repair.^{8,12} The current study investigated the use of autologous chondrocytes in order to eliminate potential host immune reaction to allogeneic cells. Although autologous cells do not incite an immune response, this cell source is not without concerns. Donor site morbidity is a major problem in human autologous chondrocyte implantation.²³ In our case, 1.5–2.5 g of cartilage was removed from the distal talus and although these donor sites are non-weight-bearing surfaces in the horse, such extensive cartilage debridement risks long-term negative effects in the joint. Additionally, the expansion of chondrocytes in culture following cartilage digestion is associated with dedifferentiation and loss of the chondrocyte phenotype.^{24–26} It is difficult to find an ideal balance between limiting the amount of cartilage harvested in order to decrease donor site morbidity, while simultaneously obtaining enough tissue that extensive expansion, and thereby dedifferentiation, is not required to attain adequate cell numbers for implantation. It is worth noting that redifferentiation of chondrocytes has been shown to occur rapidly in three-dimensional cultures²⁷ and could be expected to occur in the fibrin complexes used in this study.

The minimally invasive nature of chondrocyte implantation in this study is a major advantage of this technique. Transduced chondrocytes were securely implanted into full-thickness chondral defects using a self-polymerizing cell/fibrinogen mixture and calcium-activated thrombin under arthroscopic guidance. Eliminating the need for an arthrotomy to graft cartilage defects decreases postoperative morbidity and healing times. Although both cartilage harvest and chondrocyte implantation were performed using minimally invasive techniques, donor site morbidity and need for a second surgery are ongoing concerns. Considering the potential detrimental consequences of cartilage harvest, alternative cell sources for cartilage repair, such as chondrogenically differentiated stem cells may provide a superior treatment method. Additionally, scaffoldless bioengineered neocartilage may represent an optimal strategy for maintaining the chondrocyte

phenotype during *in vitro* culture, while providing an integrative, mechanically sound, and biocompatible repair tissue.²⁸

This well-established equine model likely provides the closest approximation to cartilage repair in man and is a more robust model than commonly used small animal models. The cartilage of the equine lateral trochlear ridge has approximately the same thickness (2–3 mm) and load-bearing characteristics as human femoral condyles.²⁹ Conversely, the expense of large animal studies can limit animal numbers in experimental groups, making a power analysis vital during study design. Here, experimental groups of eight horses gave a statistical power of greater than 90%. Interanimal variability plays an important role in gene therapy; host differences can affect transduction efficiency, transgene expression, and survival of transduced cells. In this study, we observed moderate interanimal variability; however, the significant effects of IGF-I transduced chondrocyte implantation were readily apparent.

Although improved healing was noted in defects implanted with IGF-I gene transduced chondrocytes, the ultimate aim of reliable hyaline cartilage repair throughout the entire defect depth was not achieved. At 8 months postimplantation, graft–host integration was complete in histological sections from some but not all treated defects, which would likely limit durability of the repair tissue. It is possible that longer-term evaluation of the grafts may have shown enhanced integration. Although full integration was not observed, it is noteworthy that all grafts remained stable throughout the 8-month study period, during which horses had free access to exercise placing substantial load and stress on the repair tissue. Quantitative analysis indicated defects grafted with chondrocytes expressing IGF-I were smoother and had improved collagen type II content. However, the repair was not consistently smooth (**Figure 2a**) and collagen type II did not appear to be evenly distributed (**Figure 2e**). This may have been due to differences in transgene expression of transduced chondrocytes throughout the depth of the implant. The superficial layer of the repair tissue undergoes more intense wear postimplantation which could increase cell death and decrease ECM production.

In summary, minimally invasive implantation of autologous chondrocytes transduced *ex vivo* with rAAV5-IGF-I improved long-term healing of full-thickness chondral defects in the equine model. Hallmark features of hyaline-like repair tissue were noted in chondrocyte-IGF-I treated lesions, including hyaline-like tissue architecture and an increased abundance of collagen type II. Importantly, rAAV5 transduced chondrocytes appeared to have little adverse effect on joints as there were no significant alterations in synovial fluid composition, no significant differences noted in synovial biopsies, and all treated horses remained physically and clinically sound. Although this study showed improved repair with genetically modified chondrocytes, return of native cartilage characteristics was not consistent and remains a significant challenge. Further investigation into genetically enhanced chondrocytes that concurrently limit catabolic cytokine abundance may improve the hyaline character of the repair more profoundly.

MATERIALS AND METHODS

Adeno-associated vectors. Full-length equine IGF-I cDNA was amplified by PCR. Equine IGF-I cDNA and GFP were each subcloned into the rAAV transfer plasmid pHpa-trs-SK using *SacII* and *NotI* sites. The transgenes

were flanked by inverted terminal repeats and under control of the CMV promoter. scAAV5-IGF-I and scAAV5-GFP vectors were generated by the Research Vector Core at The Children's Hospital of Philadelphia in HEK293 cells using the triple plasmid transfection method in which cells were transfected with three different plasmids. The plasmids included: (i) rAAV-IGF-I or rAAV-GFP construct, (ii) the AAV *rep* and *cap* genes, and (iii) the adenovirus helper virus.

Cartilage biopsy and graft preparation. Twenty-four horses, between 2 and 4 years old (mean = 2.9 years) and free of hindlimb musculoskeletal disease underwent cartilage biopsy using a protocol approved by the Institutional Animal Care and Use Committee. Briefly, horses were anesthetized and articular cartilage (1.5–2.5 g) was arthroscopically harvested from the non-weight-bearing portions of the distal medial and lateral trochlear ridges of one randomly selected talus. Chondrocytes were isolated, cultured under monolayer conditions to 20×10^6 cells, and then kept frozen in liquid nitrogen as previously described.³⁰ Chondrocytes were prepared for surgical implantation as previously described,³¹ however, cells were transduced 48 hours prior to surgery in Opti-Mem (Invitrogen, Grand Island, NY) with rAAV5-IGF-I, rAAV5-GFP, or no virus as a negative control at a dose of 10^5 vg/cell for 2 hours. Following transduction, chondrocytes were suspended in cryoprecipitated autogenous fibrinogen that was prepared from previously collected plasma.³²

Chondrocyte implantation. Horses were anesthetized, synovial fluid was collected from both femoropatellar joints, and bilateral arthroscopy was performed. A full-thickness chondral defect that extended down to, but not through, the subchondral plate, was created on the lateral trochlear ridge of both femurs using a 15 mm diameter fluted spade-bit cutter with a sharpened perimeter skirt (Special Devices, Grass Valley, CA) under arthroscopic guidance. Residual cartilage and calcified cartilage were removed using a loop curette. Each horse served as its own control with one defect being grafted with chondrocyte/fibrinogen mixture and the contralateral defect grafted with fibrin alone. Chondrocyte implantation was performed using helium gas for joint distension. A double-barreled syringe containing the fibrinogen/chondrocyte mixture in one syringe and calcium-activated bovine thrombin (500 U/ml; Sigma, St Louis, MO) in the other syringe to polymerize the fibrinogen was used, providing an adhesive clot of chondrocytes. Once the clot became firm, the joint was lavaged with sterile fluid and put through repeated range of motion to visually confirm retention of the graft. Perioperative pain management was achieved through use of epidural morphine and oral phenylbutazone administration. Horses were box stall rested for 4 weeks postoperatively, followed by 4 weeks of increasing amounts of walking.

Synovial fluid collection and analysis. Synovial fluid was collected from both femoropatellar joints immediately preoperatively and then at days 4, 7, 14, 28, 56, and 224 postimplantation. Cytological analysis of the synovial fluid was performed with total and differential leukocyte count performed by Coulter (Beckman Coulter, Fullerton, CA), and smear evaluation performed on Giemsa-stained slides (LIDE Laboratories, Florissant, MO). Synovial fluid was also analyzed for IGF-I concentration using an ELISA (Quantikine; R&D Systems, Minneapolis, MN).

Arthroscopic evaluation at 8 weeks postimplantation. Eight weeks post-implantation surgery, arthroscopic second look examination of defects in both joints was performed. The defects were examined, photographed, and graded by two blinded observers (A.J.N. and K.O.) (**Table 1**), and pathology scores were averaged for statistical analysis. The following parameters were evaluated: defect fill, amount of smooth repair tissue covering defect, whiteness of repair tissue, graft–recipient tissue integration (assessed by applying pressure to defect perimeter using an arthroscopic probe), and degree of subchondral bone attachment (assessed using an arthroscopic probe). Following defect evaluation, a synovial biopsy was taken and fixed in 4% paraformaldehyde for histology. Exercise was restricted to box stall

rest for 2 weeks, and then, horses were allowed free pasture turnout for the remainder of the study period.

Gross evaluation and specimen collection. Eight months postimplantation horses were euthanized with a barbiturate overdose. The popliteal and inguinal lymph nodes were collected and fixed. The lateral trochlear ridges were exposed, photographed, and graded using the same semiquantitative scoring system used at 8-week arthroscopy (Table 1). An oscillating saw was used to remove a 5-mm-wide rectangular osteochondral block containing the middle third of the repair tissue and extending 5 mm beyond the proximal and distal edges of the graft. The blocks were fixed in 4% paraformaldehyde and then decalcified in 10% ethylenediamine-tetra-acetic acid in preparation for histology and immunohistochemistry. Repair tissue from the medial third of the defect was harvested, along with a 5-mm-wide strip of perilesion cartilage and remote cartilage from the medial trochlear ridge. These tissues were snap-frozen in liquid nitrogen and stored in -80°C for later gene expression and biochemical analysis. A 3×10 mm biopsy of the synovial membrane and underlying joint capsule was collected from the cranial aspect of the femoropatellar joint and fixed in 4% paraformaldehyde.

Morphologic analysis

Histology. Decalcified osteochondral blocks were embedded in paraffin, sectioned at $6\ \mu\text{m}$, and stained with hematoxylin and eosin to evaluate morphology, and toluidine blue to evaluate proteoglycan content and distribution in the ECM. Stained osteochondral blocks were graded by two investigators (A.J.N. and K.O.) using the semi-quantitative scoring system in Table 1. The following histological parameters were assessed: defect fill, predominance of chondrocyte cell type, perilesional cloning, graft-recipient tissue integration, subchondral bone attachment, surface fibrillation, tidemark reformation, toluidine blue staining, and collagen type II predominance. Synovial membrane was sectioned and stained with hematoxylin and eosin for scoring. Popliteal and ileofemoral lymph nodes collected from both limbs were also stained with hematoxylin and eosin and scored by a veterinary pathologist. The B-cell domain, T-cell domain, medullary cords, and medullary sinuses were evaluated for inflammatory reaction.

Collagen type II immunohistochemistry. Osteochondral sections were deparaffinized, rehydrated, and treated with $5\ \mu\text{g}/\text{ml}$ hyaluronidase (Sigma-Aldrich, St Louis, MO) at 37°C for 60 minutes prior to blocking with normal goat serum. Sections were then incubated with polyclonal rat anti-bovine type II collagen primary antibody (1:100) (courtesy of Dr Micheal Cremer, VA Hospital, Memphis, TN). A secondary biotinylated goat-anti-rat (ABC Staining System; Santa Cruz Biotechnology, Dallas, TX) was applied to sections, followed by streptavidin-conjugated peroxidase to catalyze chromagen development in 3,3'-diaminobenzidine tetrachloride (Sigma-Aldrich). Sections were counterstained with hematoxylin and scored based on amount and intensity of staining (Table 1).

Biochemical analyses. Frozen lesion, perilesion, and remote tissues were pulverized in liquid nitrogen in a freezer mill (6750 Freezer Mill; Spex Certiprep, Metuchen, NJ), lyophilized, and used for glycosaminoglycan, DNA, and type II collagen assays. The dimethylmethylene blue spectrophotometric assay was used to estimate proteoglycan content in tissues. Chondroitin-4 sulfate was used to establish a standard curve, and the optical density determined at $525\ \text{nm}$.³³ Total DNA content was determined from papain digested tissues that were incubated for 24 h at 65°C and then mixed with bisbenzimidazole compound (compound 33258, Hoechst; Sigma-Aldrich) for quantification by fluorometric assay, using an excitation wavelength of $348\ \text{nm}$ and an emission wavelength of $456\ \text{nm}$. Calf thymus DNA was used to establish a standard curve. Collagen type II content was assessed using a multispecies collagen type II ELISA (Chondrex, Redmond, WA). Lyophilized cartilage was pretreated and digested with guanidine, pepsin, and elastase prior to assay by ELISA. The optical density values were read at $490\ \text{nm}$.

Gene expression analysis. Following pulverization in a freezer mill, tissues were mechanically homogenized, and RNA was isolated from tissues using the PerfectPure RNA Tissue Kit (5 Prime, Gaithersburg, MD). Purity and concentration of the RNA was assessed by UV microspectrophotometry (NanoDrop 2000 Spectrophotometer; Thermo Scientific, Waltham, MA). Gene expression was quantified by real-time PCR using the Taqman One-Step RT-PCR technique (Absolute Quantitative PCR; ABI PRISM 7900 HT Sequence Detection System; Applied Biosystems, Foster City, CA). Gene expression of IGF-I, collagen type II, aggrecan, and collagen type I was measured in lesion, perilesion, and remote tissue. All samples were run in duplicate. Primer Express Software Version 2.0 (Applied Biosystems) was used to design equine primers and dual-labeled fluorescent probes (6-carboxyfluorescein as the 5' label (reporter dye) and 5-carboxymethylrhodamine as the 3' label (quenching dye)) (Supplementary Table S1). The total copy number of mRNA was determined using a validated standard curve, and these values were normalized to the housekeeping gene 18S.

Statistical analysis. Each horse in the study provided multiple observations; one chondral defect filled with (i) rAAV5-IGF-I chondrocytes, (ii) rAAV5-GFP chondrocytes, or (iii) naive chondrocytes, and the contralateral defect filled with fibrin vehicle. Several of the outcome parameters (e.g., synovial fluid IGF-I concentration) were also repeatedly measured over time. In order to account for possible correlation between observations made in the same horse, a mixed effects model was used for analysis. Horse was treated as a random effect and day and treatment were treated as fixed effects with an interaction term for day and treatment. Day was treated as a categorical variable to allow for the nonlinear effect of time. Continuous data that did not appear to have a Gaussian distribution were transformed using the natural logarithm. Multiple comparisons for differences in parameters for each interaction were made with a Tukey's *post hoc* test or Bonferroni correction. Specific linear contrasts were fitted to the model where appropriate to examine the nature of the interactions. Statistical analysis was performed using JMP. The level of significance was set at $P < 0.05$.

SUPPLEMENTARY MATERIAL

Figure S1. Quantitative polymerase chain reaction (qPCR) data.

Table S1. Equine primer and probe sequences used to analyze gene expression.

ACKNOWLEDGMENTS

This research was supported by National Institute of Health 5R01-AR055373 (A.J.N.). The authors acknowledge Dr Sean McDonough for his assistance with assessment of lymph node biopsies, Ms Bethany Austin for her assistance with animal care, and Ms Mary Lou Norman for her assistance with histology.

REFERENCES

- Jackson, DW, Lalor, PA, Aberman, HM and Simon, TM (2001). Spontaneous repair of full-thickness defects of articular cartilage in a goat model. A preliminary study. *J Bone Joint Surg Am* **83-A**: 53–64.
- Martin, JA and Buckwalter, JA (2003). The role of chondrocyte senescence in the pathogenesis of osteoarthritis and in limiting cartilage repair. *J Bone Joint Surg Am* **85-A** (suppl. 2): 106–110.
- Nehrer, S, Spector, M and Minas, T (1999) Histologic analysis of tissue after failed cartilage repair procedures. *Clin Orthop Relat Res* **365**: 149–162.
- Steadman, JR, Rodkey, WG and Briggs, KK (2002). Microfracture to treat full-thickness chondral defects: surgical technique, rehabilitation, and outcomes. *J Knee Surg* **15**: 170–176.
- Hangody, L, Kish, G, Kárpáti, Z, Szerb, I and Udvarhelyi, I (1997). Arthroscopic autogenous osteochondral mosaicplasty for the treatment of femoral condylar articular defects. A preliminary report. *Knee Surg Sports Traumatol Arthrosc* **5**: 262–267.
- Marcacci, M, Kon, E, Zaffagnini, S, Filardo, G, Delcogliano, M, Neri, MP *et al.* (2007). Arthroscopic second generation autologous chondrocyte implantation. *Knee Surg Sports Traumatol Arthrosc* **15**: 610–619.
- Basad, E, Ishaque, B, Bachmann, G, Stürz, H and Steinmeyer, J (2010). Matrix-induced autologous chondrocyte implantation versus microfracture in the treatment of cartilage defects of the knee: a 2-year randomised study. *Knee Surg Sports Traumatol Arthrosc* **18**: 519–527.
- Goodrich, LR, Hidaka, C, Robbins, PD, Evans, CH and Nixon, AJ (2007). Genetic modification of chondrocytes with insulin-like growth factor-1 enhances cartilage healing in an equine model. *J Bone Joint Surg Br* **89**: 672–685.

9. Elves, MW and Zervas, J (1974). An investigation into the immunogenicity of various components of osteoarticular grafts. *Br J Exp Pathol* **55**: 344–351.
10. Adkisson, HD, Milliman, C, Zhang, X, Mauch, K, Maziarz, RT and Streeter, PR (2010). Immune evasion by neocartilage-derived chondrocytes: implications for biologic repair of joint articular cartilage. *Stem Cell Res* **4**: 57–68.
11. Verschure, PJ, van Marle, J, Joosten, LA and van den Berg, WB (1995). Chondrocyte IGF-1 receptor expression and responsiveness to IGF-1 stimulation in mouse articular cartilage during various phases of experimentally induced arthritis. *Ann Rheum Dis* **54**: 645–653.
12. Fortier, LA, Mohammed, HO, Lust, G and Nixon, AJ (2002). Insulin-like growth factor-I enhances cell-based repair of articular cartilage. *J Bone Joint Surg Br* **84**: 276–288.
13. Fortier, LA, Lust, G, Mohammed, HO and Nixon, AJ (1999). Coordinate upregulation of cartilage matrix synthesis in fibrin cultures supplemented with exogenous insulin-like growth factor-I. *J Orthop Res* **17**: 467–474.
14. Tyler, JA (1989). Insulin-like growth factor 1 can decrease degradation and promote synthesis of proteoglycan in cartilage exposed to cytokines. *Biochem J* **260**: 543–548.
15. Fosang, AJ, Tyler, JA and Hardingham, TE (1991). Effect of interleukin-1 and insulin like growth factor-1 on the release of proteoglycan components and hyaluronan from pig articular cartilage in explant culture. *Matrix* **11**: 17–24.
16. Ortvad, KF, Nixon, AJ, Mohammed, HO and Fortier, LA (2012). Treatment of subchondral cystic lesions of the medial femoral condyle of mature horses with growth factor enhanced chondrocyte grafts: a retrospective study of 49 cases. *Equine Vet J* **44**: 606–613.
17. Daya, S and Berns, KI (2008). Gene therapy using adeno-associated virus vectors. *Clin Microbiol Rev* **21**: 583–593.
18. McCarty, DM, Monahan, PE and Samulski, RJ (2001). Self-complementary recombinant adeno-associated virus (scAAV) vectors promote efficient transduction independently of DNA synthesis. *Gene Ther* **8**: 1248–1254.
19. Begum, L, Ortvad, KF and Nixon, AJ (2010). AAV-5 provides more efficient transgene expression in chondrocytes grown in adherent and suspension culture. *Trans Orthop Res Soc 56th Ann Mtg*, Seattle, WA.
20. Madry, H, Padera, R, Seidel, J, Langer, R, Freed, LE, Trippel, SB *et al.* (2002). Gene transfer of a human insulin-like growth factor I cDNA enhances tissue engineering of cartilage. *Hum Gene Ther* **13**: 1621–1630.
21. Nixon, AJ, Saxer, RA and Brower-Toland, BD (2001). Exogenous insulin-like growth factor-I stimulates an autoinductive IGF-I autocrine/paracrine response in chondrocytes. *J Orthop Res* **19**: 26–32.
22. Fortier, LA, Nixon, AJ and Lust, G (2002). Phenotypic expression of equine articular chondrocytes grown in three-dimensional cultures supplemented with supraphysiologic concentrations of insulin-like growth factor-1. *Am J Vet Res* **63**: 301–305.
23. Pearce, SG, Hurtig, MB, Clarnette, R, Kalra, M, Cowan, B and Miniaci, A (2001). An investigation of 2 techniques for optimizing joint surface congruency using multiple cylindrical osteochondral autografts. *Arthroscopy* **17**: 50–55.
24. Shakibaei, M, Seifarth, C, John, T, Rahmzadeh, M and Mobasher, A (2006). Igf-I extends the chondrogenic potential of human articular chondrocytes *in vitro*: molecular association between Sox9 and Erk1/2. *Biochem Pharmacol* **72**: 1382–1395.
25. Barbero, A, Grogan, S, Schäfer, D, Heberer, M, Mainil-Varlet, P and Martin, I (2004). Age related changes in human articular chondrocyte yield, proliferation and post-expansion chondrogenic capacity. *Osteoarthritis Cartilage* **12**: 476–484.
26. Oshin, AO, Caporali, E, Byron, CR, Stewart, AA and Stewart, MC (2007). Phenotypic maintenance of articular chondrocytes *in vitro* requires BMP activity. *Vet Comp Orthop Traumatol* **20**: 185–191.
27. Takahashi, T, Ogasawara, T, Asawa, Y, Mori, Y, Uchinuma, E, Takato, T *et al.* (2007). Three-dimensional microenvironments retain chondrocyte phenotypes during proliferation culture. *Tissue Eng* **13**: 1583–1592.
28. Schubert, T, Anders, S, Neumann, E, Schölmerich, J, Hofstädter, F, Grifka, J *et al.* (2009). Long-term effects of chondrospheres on cartilage lesions in an autologous chondrocyte implantation model as investigated in the SCID mouse model. *Int J Mol Med* **23**: 455–460.
29. Frisbie, DD, Cross, MW and McIlwraith, CW (2006). A comparative study of articular cartilage thickness in the stifle of animal species used in human pre-clinical studies compared to articular cartilage thickness in the human knee. *Vet Comp Orthop Traumatol* **19**: 142–146.
30. Nixon, AJ, Lust, G and Vernier-Singer, M (1992). Isolation, propagation, and cryopreservation of equine articular chondrocytes. *Am J Vet Res* **53**: 2364–2370.
31. Hidaka, C, Goodrich, LR, Chen, CT, Warren, RF, Crystal, RG and Nixon, AJ (2003). Acceleration of cartilage repair by genetically modified chondrocytes over expressing bone morphogenetic protein-7. *J Orthop Res* **21**: 573–583.
32. Dresdale, A, Rose, EA, Jeevanandam, V, Reemtsma, K, Bowman, FO and Malm, JR (1985). Preparation of fibrin glue from single-donor fresh-frozen plasma. *Surgery* **97**: 750–755.
33. Farndale, RW, Sayers, CA and Barrett, AJ (1982). A direct spectrophotometric microassay for sulfated glycosaminoglycans in cartilage cultures. *Connect Tissue Res* **9**: 247–248.